Dalton Transactions

Accepted Manuscript

ROYAL SOCIETY OF CHEMISTRY

www.rsc.org/dalton

Co-ordination Behaviour of a Novel Tristhiourea Tripodal Ligand; Structural variations in a series of Transition Metal Complexes

Fawaz A. Saad[a,b], James C. Knight[b], Benson M. Kariuki[b], Angelo J. Amoroso,*[b]

[a] *Umm Al-Qura University, Kingdom of Saudi Arabia. E-mail: fasaad@uqu.edu.sa*

[b] *School of Chemistry, Cardiff University, Cardiff, UK. E-mail: amorosoaj@cf.ac.uk*

†CCDC 948550–948556. For crystallographic data in CIF or other electronic format see DOI: 10.1039/

The co-ordination chemistry of a tristhiourea tris(2-pyridylmethyl)amine ligand (L^1) with a series of transition metal ions has been investigated. Crystallographic data show that large metal ions, with no geometrical preferences , such as Mn(II) and Cd(II), will form seven co-ordinate monocapped octahedral complexes, while smaller metal ions such as Zn(II) favour five co-ordinate trigonal bipyramidal structures. In a similar manner to the related bisthiourea complexes, the Ni(II) complex shows a strong preference for octahedral geometries resulting in the ligand binding asymmetrically. Spectroscopic (IR and NMR), spectrometric (MS) as well as electrochemical data for these complexes are reported.

Introduction

There is great interest in the design and synthesis of anion receptors due to their significance in developing chemical sensors and membranes for selective transport and separation of anions.[1-6] The formation of metal complexes which can selectively bind anions has attracted interest due to their potential to offer a three dimensional scaffold from which suitable hydrogen bonding groups may be positioned.[7] The work of Beer [8,9] has been at the forefront of such studies and recently, their work has included anion-templated synthesis of interlocked supramolecular structures[10] and conversely the anion binding of interlocked supramolecular structures.[11] Similarly, Leigh has show the extremely high affinity of a central cavity of a molecular knot for halides.[12] Steed has also designed anion receptors based on tripodal molecules derived from 1,3,5-substituted arene groups with additional positive charges which further enhance anion binding.[13]

Previously the use of urea[14,15,16] and thiourea[17,18] has been shown to be effective for anion binding and placing these moeities in a geometrically well defined array may induce some specificity in anion binding. Reinaud and Jabin have shown how the cavity within a calix[6]arene may be modified with urea and thiourea groups or the formation of biscalix[6]arenes with thiourea and urea linkers produce receptors for anions[19] and more specifically for phosphatidylcholine lipids.[20] Other systems with similar properties has been reviewed by Smith.[21] Recently, we have developed new tripodal ligands bearing thiourea groups on the ligand periphery and have also investigated structural aspects of related amido containing tripods.[22, 23]

Previously, we synthesised a derivative of the TPA ligand containing benzoylthiourea groups on two of the three donor arms (Figure 1, $\mathbf{L^2}$).[22] The ligand readily co-ordinated to a variety of transition metal ions and some complexes were able to co-ordinate organic dicarboxylates, such as succinic acid.

Furthermore, the nature of this interchangeable metal ion allows for an array of potential anion binders to be synthesised and these species may have varying charge and stereochemistry as we change the metals oxidation state.

In this paper, we wish to report the synthesis and characterization of a series of transition metal complexes formed from the tristhiourea tripodal ligand, L^1. We anticipated such complexes to have a C_3 symmetry making them suitable for the binding of tetrahedral anions such as perchlorate or phosphate. However, to assist in the interpretation of future anion binding experiments it is necessary to elucidate the structure and stability of each complex as the metal ion is varied. This is an important consideration as metals with strong tendancies for octahedral geometries may force the ligand to adopt an arrangement which prevents some anions from binding to the complex. Conversely, metal ions with no geometric preference may lead to the formation of a suitable anion binding cavity but a labile arrangement may lead to a lack of specificity for a given anion. This work investigates the structural properties of a series of metal ions coordinated to the tris benzoylthiourea ligand $\mathbf{L^1}$, identifying the geometrical preference of various metal centres with varying d-electron configuration.

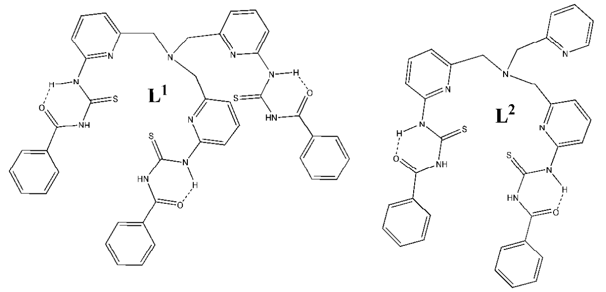

Figure 1: The tristhiourea compound under investigation, $\mathbf{L^1}$ and the related bisthiourea ligand, $\mathbf{L^2}$.

Experimental

General

NMR spectra were measured on a Bruker AM 250-400 MHz or Bruker Av-500 MHz Plus FT-NMR spectrometer. Residual signals of solvent were used for reference for ^1H and ^{13}C NMR. For infrared spectra, each compound was pressed into a disk with an excess of dried KBr and measured on a Jasco 660 FT-IR spectrophotometer. Electrospray (ES) and high-resolution (HR) mass spectra were measured on a Waters LCT Premier XE (oa-TOF) mass spectrometer. UV-Vis absorption spectra were run in HPLC grade acetonitrile (Fisher) and measured on a Jasco V-570 spectrophotometer from 230 to 1,100 nm (optical path length 1.0 cm). Elemental analyses were carried out both by the Warwick Analytical Service, University of Warwick. Tris(6-amino-2-pyridylmethyl)amine (TAPA), was prepared as reported by Harata *et al*. and Jitsukawa *et al*.[24, 25] Cyclic voltammetry was carried out using an AUTOLAB PGSTAT12 potentiostat with General Purpose Electrochemical System software (GPES version 4.7 for Windows) using a three-electrode glass cell with a Teflon-coated cell cap. A Bioanalytical platinum working electrode (model no. MF2013) a platinum wire counter electrode and a $Ag/AgNO_3$ reference electrode were used. A 0.1 M $[Bu_4N][PF_6]$ solution in CH_3CN was used as supporting electrolyte. In all cases, ferrocene was used as an internal reference. Solutions were degassed with nitrogen and a nitrogen atmosphere was maintained over the solution during the experiment.

Tristhiourea L^1

TAPA (3.401 g, 10.139 mmol) was dissolved in EtOH (200 mL) and benzoyl isothiocyanate (4.90 mL, 30. mmol) was added drop wise. The mixture was heated to 40°C for 30 minutes then allowed to cool to room temperature. The solvent volume was reduced by 50% under reduced pressure and ether was added to precipitate the brown solid product (3.147 g, 37.7 %). $C_{42}H_{36}N_{10}O_3S_3$; ^{1}H-NMR δH (400 MHz; $CDCl_3$): 3.80(6H, s); 7.39-7.43(9H, m, Ar); 7.53(3H, m, Ar); 7.69(3H, t, Ar, J=7.8Hz); 7.77(6H, d, Ar, J=6.6Hz); 8.61(3H, d, Ar, J=4.1Hz); 8.87(3H, s, NH); 12.96(3H, s, NH). ^{13}C δ_C (62.5 MHz; $CDCl_3$): 59.6, 114.1, 120.8, 127.5, 129.1, 131.6, 133.6, 138.1, 150.3, 150.4, 166.2, 176.7. Accurate ESMS (*m/z*): 825.2249 (100) $[L+H]^+$. [calculated 824.2134]. IR KBr/cm^{-1}: ν =3414br, 3053br, 1674s, 1598s, 1454s, 1331s, 755s. UV/Vis [λ_{max}, nm (ε, M^{-1}cm^{-1})] in THF: 268(106600), 288(94200) 310(58100).

General Procedure for the synthesis of metal complexes

Ligand L^1 (1 equivalent, typically 80 μmol) was dissolved in the minimum amount of $CHCl_3$ or THF (typically 3 mL). The solutions were warmed to 60˚C to ensure that the ligand fully dissolved. To this stirring solution, the metal perchlorate salt (1 equivalent), dissolved in THF or acetonitrile (2 mL), was added dropwise. Recrystallisation of the compounds typically involved the filtration of the reaction solution through celite, followed by the diffusion of diethyl ether into the solvent mixture. The isolated yields from these reactions were low to high (7-69%) depending upon the solubility of the product. This crystalline material was subsequently used for all spectroscopic measurements.

WARNING: *Perchlorate salts of metal complexes are potentially explosive. Care should be taken while handling such complexes.*

$[MnC_{42}H_{36}N_{10}O_3S_3][ClO_4]_2$ (1): Colourless plate crystals (37% yield); Accurate ESMS (*m/z*): 878.1416 (100) $[Mn(L^1)-H]^+$ [calculated 878.1436]; $MnC_{42}H_{36}N_{10}O_3S_3(CH_3CN)(ClO_4)_2$ (Found: C, 47.36; H, 3.55; N, 13.86. requires C, 47.22; H, 3.51; N, 13.77%); IR KBr/cm^{-1}: ν = 3432br, 1608s, 1532m, 1455s, 1262s, 1086s, 706s, 622s.

$[CoC_{42}H_{36}N_{10}O_3S_3][ClO_4]_2$ (2): Dark red glassy solid (40% yield); Accurate ESMS (m/z): 882.1358 (60), $[Co(L^1)-H]^+$ [calculated 882.1388]; $CoC_{42}H_{36}N_{10}O_3S_3(ClO_4)_2$ (Found: C, 46.55; H, 3.31; N, 12.88. requires C, 46.62; H, 3.35; N, 12.95%); IR KBr/cm^{-1}: ν = 3419br, 1613s, 1539m, 1447m, 1263s, 710s, 1087s, 626s; UV/Vis [λ_{max}, nm (ε, M^{-1}cm^{-1})] in CH_3CN: 260(20500), 290(14300), 310(18000), 350(6600), 500(135), 630(35), 960(2).

$[NiC_{42}H_{36}N_{10}O_3S_3][ClO_4]_2$ (3): Green needle crystals (69% yield); Accurate ESMS (m/z): 881.1411 (90), $[Ni(L^1)-H]^+$ [calculated 881.1409]; $NiC_{44}H_{39}N_{11}O_3S_3(H_2O)_{0.5}(CH_3CN)_{3.5}(ClO_4)_2$ (Found: C, 48.12; H, 4.20; N, 15.99. requires C, 48.05; H, 3.99; N, 15.94%); IR KBr/cm^{-1}: ν= 3464br, 1616s, 1539m, 1488s, 1261s, 707s, 1082s, 622s; UV/Vis [λ_{max}, nm (ε, M^{-1}cm^{-1})] in CH_3CN: 260(43950), 280(36435), 320(265000), 395(2000), 560(15), 795(10), 850(10), 1096(16).

$[CuC_{42}H_{36}N_{10}O_3S_3][ClO_4]_2$ (4): Green glassy solid (62% yield); Accurate ESMS (m/z): 886.1367 (100), $[Cu(L^1)-H]^+$ [calculated 886.1352]; $CuC_{42}H_{36}N_{10}O_3S_3(ClO_4)_2$ (Found: C, 46.36; H, 3.33; N, 12.85. requires C, 46.44; H, 3.34; N, 12.90%). IR KBr/cm^{-1}: ν = 3448br, 1610s, 1523m, 1480s, 1261s, 709s, 1088s, 621s. UV/Vis [λ_{max}, nm (ε, M^{-1}cm^{-1})] in CH_3CN: 242(35700), 262(40825), 287(31580), 311(27535), 430(900), 621(60), 975(10).

$[ZnC_{42}H_{36}N_{10}O_3S_3][ClO_4]_2$ (5): Colourless needle crystals (24% yield); ^{1}H-NMR (400 MHz; CD_3CN): 4.41(6H, s); 7.49(6H, t, Ar, J=7.8Hz); 7.59(3H, d, Ar, J=7.8Hz); 7.69(6H, t, Ar, J=8.0Hz); 7.78(6H, d, Ar, J=7.5Hz); 8.23(3H, d, Ar, J=7.9Hz); 10.23(3H, s, NH); 13.39(3H, s, NH); ^{13}C δ_C (62.5 MHz; CD_3CN): 56.7, 123.2, 124.5, 129.5, 129.7, 131.7, 135.0, 144.5, 151.5, 155.0, 170.0, 180.7; Accurate ESMS (*m/z*): 887.1473 (100) $[Zn(L^1)-H]^+$ [calculated 887.1347]; $ZnC_{42}H_{36}N_{10}O_3S_3(CHCl_3)(CH_3CN)(ClO_4)_2$ (Found: C, 43.29; H, 3.17; N, 12.13%. requires C, 43.37; H, 3.23; N, 12.37%); IR KBr/cm^{-1}: ν= 3437br, 1623s, 1522s, 1447s, 1261s, 711s, 1094s, 622s.

$[CdC_{42}H_{36}N_{10}O_3S_3][ClO_4]_2$ (6): Colourless plate crystals (7% yield); ^{1}H-NMR (500 MHz; CD_3CN): 4.20(6H, s); 7.38(3H, d, Ar, J=7.5Hz); 7.51(3H, d, Ar, J=7.5Hz); 7.57(3H, t, Ar, J=7.6Hz); 7.58(3H, t, Ar, J=7.5Hz); 7.76(3H, t, Ar, J=7.5Hz); 7.92(3H, d, Ar, J=7.9Hz); 7.94(3H, d, Ar, J=7.9Hz); 8.12(3H, t, Ar, J=7.8Hz) 10.27(3H, s, NH); 13.60(3H, s, NH); ^{13}C δ_C (78 MHz; CD_3CN): 57.9, 122.3, 124.9, 129.6, 129.9, 131.9, 135.3, 143.3, 151.2, 154.0, 170.5, 181.1; Accurate ESMS (*m/z*): 937.1226 (30), $[Cd(L^1)-H]^+$ [calculated 937.1089], 469.0505 (20), $[Cd(L^1)/2]^+$ [calculated 469.0584]; $CdC_{42}H_{36}N_{10}O_3S_3(H_2O)_{0.5}(ClO_4)_2$ (Found: C, 43.81; H, 3.17; N, 12.02. requires C, 44.04; H, 3.25; N, 12.22%); IR KBr/cm^{-1}: ν = 3450br, 1601s, 1522s, 1451s, 1263s, 706m, 1107s, 620s.

Results and Discussion

Synthesis of Ligand and Complexes

The amino groups of the TAPA ligand were converted into thiourea groups via the dropwise addition of 3 equivalents of benzoyl-isothiocyanate in ethanol with continuous stirring and gentle heating.[26] Following this addition, the reaction mixture changed from a clear yellow solution to a light brown suspension allowing the product to be isolated by filtration and washing with diethyl ether. The product has good thermal and photostability and was found to be soluble in common solvents such as chloroform or THF.

Complexes of this ligand could readily be formed by the addition of an aqueous solution of a metal salt to a THF or acetonitrile solution of the ligand. Use of the perchlorate salt, resulted in the product being precipitated from solution, facilitating product purification and isolation. In addition, it was anticipated that the perchlorate salt would not be co-ordinated to the metal centre but may interact with the thiourea moieties.

Spectroscopic Properties of Complexes

^{1}H and ^{13}C NMR

Both proton and carbon NMR were consistent with a three-fold symmetrical structure in solution. While this is consistent with the solid state structure of the Cd(II) complex, the Zn(II) species does not show C_{3v} symmetry in the solid state, with crystallographic data indicating each arm of the ligand is symmetrically independent. It is highly likely the rapid fluxional process account for the observed symmetry, similar to that observed in the free ligand. The proton NMR of both the Zn(II) and the Cd(II) complexes show very similar NH resonances (10.23 and 13.39 for Zn; 10.27 and 13.60 for Cd), perhaps suggesting that in solution both complexes interact with the perchlorate ion to a similar extent. Considering that the most sterically favourable conformation of the Zn complex does not form the anion binding cavity, it is highly likely that neither Zn or Cd complexes significantly bind the perchlorate ion in solution.

IR Spectra

A strong peak at 1331 cm^{-1}, assigned to the ν(C=S) is shifted to lower energy (1261-1263 cm^{-1}) indicating the co-ordination of the sulfur to the metal ion (Table 1). In addition, the very strong band at 1674 cm^{-1}, assigned to the ν(C=O) vibration of L^1 is shifted to lower wavenumber in all complexes. Structural data shows that the carbonyl does not directly co-ordinate to the metal centre but does form a strong hydrogen bond with an NH group causing this shift in stretching frequency. All complexes reveal two characteristic unsplit infrared active bands at ~1,100 cm^{-1} and ~622 cm^{-1} indicative of perchlorate.[27,28] All of these features are consistent with the available X-ray diffraction data for the complexes.

Table 1 IR Stretching Frequencies of Complexes of L^1 (cm^{-1})^a

Compound	ν(C=S)	ν(C=O)	ν(Cl-O)
L^1	1331(s)	1674(s)	-
1	1262(s)	1608(s)	1086(s), 622(s)
2	1263(s)	1613(s)	1087(s), 626(s)
3	1261(s)	1616(s)	1082(s), 622(s)
4	1261(s)	1610(s)	1088(s), 621(s)
5	1261(s)	1623(s)	1094(s), 622(s)
6	1263(s)	1601(s)	1107(s), 620(s)

^{a} IR spectra measured as KBr disc.

Cyclic Voltammetry

The electrochemical data of compounds **1-4** are summarised in Table 2. The cyclic voltammogram of the manganese compound, **1**, reveals two irreversible reduction processes in the cathodic region at -1.96V and -1.30V (vs Fc$^+$/Fc). By contrast, the seven co-ordinate manganese (II) complex of Mn-TPAA exhibits oxidative processes at +1.2 V and +1.7 V (*vs* SCE; 0.74V and 1.24V vs Fc/Fc$^+$).[29] As the standard potential for the aqueous Mn(III)/Mn(II) couple is 0.899V vs Fc/Fc$^+$, the observed processes is clearly not a metal-centred oxidation, and while the observed processes cannot be unequivocally ascribed they are most likely to be due to ligand-centered reductions.

The voltammogram of the Co^{II} complex, **2**, has quite similar electrochemical behaviour analogous to the Mn^{II} complex with an irreversible reduction at -2.04 V (*vs* Fc/Fc$^+$), while the nickel complex, **3**, consists of two broad irreversible waves.

Table 2: Electrochemical data for complexes **1**, **2** and **3** (CH_3CN; supporting electrolyte: $[Bu_4N][PF_6]$ (0.1 M); 20 ºC; Scan rate = 0.1 Vs^{-1}).

Compound	E_{pc}/V (ΔE, mV)^{a,}
1	-1.96, -1.30
2	-2.04
3	-1.83, -1.24,

The voltammogram of the copper compound, **4**, shows two peaks with a large peak-to-peak separation, coupled to each other. The voltammograms are suggestive of quasireversible behaviour, with cathodic and anodic processes of equal current centred at -0.37 V (Fig. 2), and the separation varying with scan rate (~675-450 mV).. The process is most likely attributable to a Cu$^{II/I}$ redox couple that exhibits slow electron-transfer kinetics, perhaps due to geometrical rearrangements associated with the change in metal oxidation state. Interestingly, the bisthiourea Cu(II) complex[12] is a five co-ordinate, trigonal pyramidal species which gives a redox couple at a similar potential to **4** (-0.35V vs Fc$^+$/Fc) but in that case it is electrochemically reversible. While this potential window is common for TPA complexes of Cu(II),[30] the quasireversibility of this complex might suggest a different co-ordination mode to the bisthiourea complex or perhaps more extensive hydrogen bonding making rearangements of the co-ordination sphere occur more slowly.

Table 3: Electronic spectral assignments for L^1 and complexes

Compound	π-π* transitions / λ (nm)	MLCT / λ (nm)	d-d transitions / λ (nm)	Δ (cm^{-1})^b
L^1	268(106600), 288(94200), 310(58100)	-	-	-
2	260(20500), 290(14300), 310 (18000)	350(6600)	500(100), 630(50), 960(2)	-
3	260(43950), 280(36435), 320(265000)	395(2000),	560(15), 795(10), 850(10) 1096(16)	9,124
4	242(35700), 262(40825), 287(31580), 311(27535)	430(900)	621(60), 975(10)	-

Performed at room temperature (**2**, **3**, **4**) in CH_3CN solution, L^1 in THF solution; Numbers in parentheses indicate molar absorption coefficients ε (M^{-1}cm^1). ^{b}values calculated by assuming an octahedral geometry .

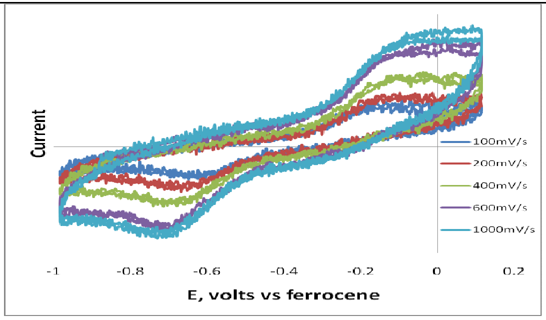

Figure 2: Cyclic voltammetry for **4** vs Fc/Fc$^+$. (Pt working electrode; 0.1 M TBAH; conc of **4** < 0.1 mM)

Electronic Absorption Spectra

The electronic spectra of L^1 and relevant complexes have been obtained and the data are presented in Table 3. The free ligand and all complexes show typical π-π* transitions at high energy (~265, ~285 and ~310 nm).

Compound **2** gives a MLCT band at 28,430 cm^{-1},similar to that observed with L^2 (25,000 cm^{-1}). While the crystal structure of **2** could not be obtained, the trigonal bipyramidal Co(II) complex of L^2 has a similar UV-vis spectrum, although in this case an additional very weak d-d peak at 960nm is observed (as would be expected for TBP complexes, $^4A_2'(F)\rightarrow{}^4E(P)$). This is suggestive of **2** having a TBP coordination geometry made up by the four nitrogen donors and one of the three sulphur donors.

Compound **3** shows a MLCT band at 25,200 cm^{-1} and four d-d transitions at 9,120 cm^{-1}, 11,750 cm^{-1}, 12,580 cm^{-1} and 17,850 cm^{-1}. The d-d transitions may be ascribed to $^3A_{2g}\rightarrow{}^3T_{2g}$, $^3A_{2g}\rightarrow{}^1E_g$, $^3A_{2g}\rightarrow{}^3T_{1g}(F)$ and $^3A_{2g}\rightarrow{}^3T_{1g}(P)$ respectively. Using these assignments yields Δ = 9,120 cm^{-1}. The analogous bisthiourea ligand has been shown to form octahedral nickel complexes which exhibits a similar N_5S environment. The co-ordination sphere of the two metal complexes is almost identical,[22] however the slightly smaller ligand field splitting of the tristhiourea compared to the bisthiourea may be due to the additional steric bulk of the third thiourea group not allowing the close approach of the pyridine donors to the metal centre.

The electronic spectrum of Cu(II), **4**, gives an electronic spectrum with a MLCT band at 23,250 cm^{-1}. In addition, the spectrum contains a very broad asymmetric peak in the visible region. There are two likely explanations. While a Jahn-Teller distortion of an octahedral centre leads to a tetragonal distortion, causing the ^2E_g term to split into $^2B_{1g}$ and $^2A_{1g}$, and the $^2T_{2g}$ term to split into $^2B_{2g}$ and ^2E_g, another possible explanation is the formation of a trigonal bipyramidal geometry. Typically, copper (II) complexes with a TBP geometry display two absoptions. Compound **4** shows two peaks (16,100 cm^{-1} and 10,250 cm^{-1}) and the low energy of these absorptions is more typical for TBP. Given the nature of the ligand, predisposed for TBP co-ordination, we have tentatively assigned this compex as trigonal bipyramidal, similar to that observed with **5**.

Crystallographic Studies

All single crystal X-ray data was collected at 150 K on a Bruker/Nonius Kappa CCD diffractometer using graphite monochromated Mo-Kα radiation (λ = 0.71073 Å), equipped with an Oxford Cryostream cooling apparatus. Crystal parameters and details of the data collection, solution and refinement are presented in Table 4. The data was corrected for Lorentz and polarization effects and for absorption using SORTAV.[31] Structure solution was achieved by direct methods (Sir-92 program system)[32] and refined by full-matrix least-squares on F2 (SHELXL-97)[33] with all non hydrogen atoms assigned anisotropic displacement parameters. Hydrogen atoms attached to carbon atoms were placed in idealised positions and allowed to ride on the relevant carbon atom. In the final cycles of refinement, a weighting scheme that gave a relatively flat analysis of variance was introduced and refinement continued until convergence was reached. Molecular structures in the figures were drawn with ORTEP-3.0 for Windows (version 2.02).[34] Relevant crystal data are given for all structures in Table 4 along with relevant bond lengths and angles in Tables 6, 8, 10, and 13

$[Mn^{II}L^1][ClO_4]_2{\cdot}CH_3CN$ (1): The manganese compound crystallises in the trigonal space group R-3:h and contains 1/3 complex within the asymmetric unit (asu). The Mn^{II} ion lies at the centre of a slightly distorted capped octahedron co-ordination geometry which is confirmed by Continuous Shape Mapping (CShM) (Table 5). The Mn^{II} ion is surrounded by three types of donor atoms: an alkyl amine nitrogen donor (N1), three pyridine moieties (N2, N5 and N8) and three sulfur donors (S1, S2 and S3)(Figs. 3 and 4). The co-ordinative bond length for the pyridyl donors is ~2.436(4) Å , the Mn-S distance is 2.6148(16) Å while the central N donor has a shorter distance of 2.276(8) Å (see Table 6). This is the first example of a complex where the Mn^{II} cation is surrounded by a N_4S_3 donor set. The related ligand L^{2},[22] despite only having six donor atoms also gives a 7 co-ordinate Mn(II) complex, with the final

INSERT TABLE 4 HERE

donor being a perchlorate counter-ion. The L^2 complex is better described as a capped trigonal prism, although it is also close to monocapped octahedral geometry (S(TPRS):0.671; S(OCF):0.831) and both the Mn-N(pyridyl) distances (av. 2.276(16) Å) and the Mn-S distances (av. 2.544(14) Å) are significantly shorter. In contrast, the C_3 symmetric ligand tris(6-pivaloylamino-2-pyridylmethyl)-amine (TPPA) yields 7 co-ordinate complexes that are clearly monocapped octahedral (S(OCF):0.33; S(TPRS):1.53),[23] similarly to $\mathbf{L^1}$ but the complex has shorter Mn-N distances (av 2.311(4) Å) as well as three short Mn-O bonds (av. 2.173(3) Å). It seems likely that for a d^5 high spin complex, the final geometry is largely determined by the steric requirements of the ligand system.

Finally, three hydrogens (on N4, $N4^{ii}$, $N4^{iii}$) are directed towards a central cavity below the metal centre where a tetrahedral perchlorate ion is held via three hydrogen bonds (Figure 5; Table 7). Similar hydrogen bonding using tripodal C_3 symmetric hydrogen bond donors for the phosphate ion has been reported by Tobey and Anslyn.[35]

Table 5: Continuous Symmetry Mapping Results for complexes **1,** and **6**

Structure	HP	HPY	PBPY	OCF	TPRS	JPBP	(JETPY)
Mn (**1**)	37.401	18.305	8.251	0.256	1.648	12.515	20.799
Cd (**6**)	37.652	17.858	8.353	0.304	1.722	12.639	20.967

HP: Heptagon (D7h), HPY: Hexagonal pyramid (C6v), PBPY: Pentagonal bipyramid (D5h), OCF: Capped octahedron (C3v), TPRS: Capped trigonal prism (C2v), JPBP: Johnson pentagonal bipyramid J13 (D5h), JETPY: Johnson elongated triangular pyramid J7 (C3v).

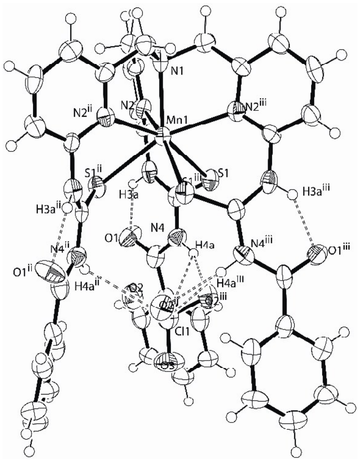

Figure 3: The asymmetric unit of **1** and the core geometry. Displacement ellipsoids are shown at 50% probability. H atoms are of arbitrary size.

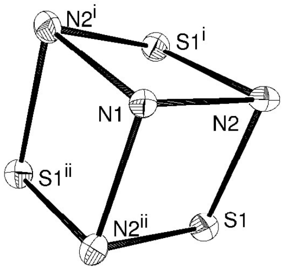

Figure 4: A view of the monocapped octahedral donor atom geometry of **1**. (The donor N1 occupying the capping position).

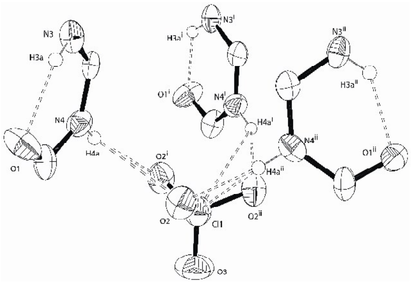

Figure 5: View of the hydrogen bonding interactions of **1**.

Table 6: Selected Bond lengths (A°) and Angles (°) for **1**

Mn(1)-N(1)	2.276(8)	Mn(1)-S(1)	2.6149(16)
Mn(1)-N(2)	2.437(4)	$Mn(1)-S(1)^{ii}$	2.6152(16)
$Mn(1)-N(2)^{ii}$	2.436(4)	$Mn(1)-S(1)^{iii}$	2.6142(16)
$Mn(1)-N(2)^{iii}$	2.435(4)		
N(1)-Mn(1)-N(2)	72.68(11)	$N(2)^{ii}-Mn(1)-S(1)^{ii}$	77.07(10)
$N(1)-Mn(1)-N(2)^{ii}$	72.68(11)	$N(2)^{ii}-Mn(1)-S(1)^{iii}$	78.44(10)
$N(1)-Mn(1)-N(2)^{iii}$	72.68(11)	$N(2)^{iii}-Mn(1)-N(2)$	111.53(10)
N(1)-Mn(1)-S(1)	125.88(4)	$N(2)^{iii}-Mn(1)-N(2)^{ii}$	111.56(10)
$N(1)-Mn(1)-S(1)^{ii}$	125.88(4)	$N(2)^{iii}-Mn(1)-S(1)$	78.43(10)
$N(1)-Mn(1)-S(1)^{iii}$	125.89(4)	$N(2)^{iii}-Mn(1)-S(1)^{ii}$	161.43(13)
N(2)-Mn(1)-S(1)	77.06(10)	$N(2)^{iii}-Mn(1)-S(1)^{iii}$	77.09(10)
$N(2)-Mn(1)-S(1)^{ii}$	78.41(10)	$S(1)-Mn(1)-S(1)^{ii}$	89.11(6)
$N(2)-Mn(1)-S(1)^{iii}$	161.40(13)	$S(1)^{iii}-Mn(1)-S(1)$	89.13(6)
$N(2)^{ii}-Mn(1)-N(2)$	111.52(10)	$S(1)^{iii}-Mn(1)-S(1)^{ii}$	89.12(6)
$N(2)^{ii}-Mn(1)-S(1)$	161.42(13)		

Table 7: H-bonding geometry (Å) for **1**

D-H…A	D-H	H…A	D…A	D-H…A
N3-H3A …O1	0.86	1.935	2.627	136.55
N4-H4A …O2	0.86	2.184	2.973	152.26

$\mathbf{[Ni^{II}L^1(CH_3CN)][ClO_4]_2 \cdot 0.5H_2O \cdot 3.5CH_3CN}$ **(3):** The nickel compound crystallises in the triclinic space group P-1 and contains a single complex within the asu (Fig. 6). The resulting complex is six-coordinate with an octahedral geometry. To achieve this geometry, only five of the seven donor atoms of the ligand co-ordinate. Two sulfur atoms do not co-ordinate and the final donor atom comes from a co-ordinated acetonitrile molecule. The geometry about the metal centre is very similar to that seen with Ni(II)-$\mathbf{L^2}$.[22] Relevant bond lengths and angles are listed in Tables 8 and 9. Also, the metal-donor distances are comparable except that **3** has one longer Ni-N bond. This difference may be assigned to the additional steric bulk of the third thiourea group; the long Ni-N bonds being associated with pyridine bearing the thiourea group not coordinated to the metal centre.

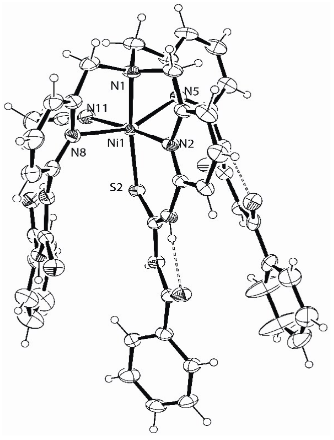

Figure 6: The asymmetric unit of **3** and the core geometry. Displacement ellipsoids are shown at 30% probability. H atoms are of arbitrary size.

Table 8: Selected Bond lengths (A°) and Angles (°) for [NiL^1]$^{+2}$ **3**

Ni(1)-N(1)	2.076(4)	Ni(1)-N(8)	2.261(4)
Ni(1)-N(2)	2.056(4)	Ni(1)-N(11)	2.051(6)
Ni(1)-N(5)	2.218(4)	Ni(1)-S(2)	2.3440(15)
N(1)-Ni(1)-N(5)	76.64(17)	N(5)-Ni(1)-S(2)	99.15(12)
N(1)-Ni(1)-N(8)	80.25(17)	N(8)-Ni(1)-S(2)	104.37(12)
N(1)-Ni(1)-S(2)	174.25(14)	N(11)-Ni(1)-N(1)	97.57(19)
N(2)-Ni(1)-N(1)	84.30(18)	N(11)-Ni(1)-N(2)	173.41(17)
N(2)-Ni(1)-N(5)	100.01(17)	N(11)-Ni(1)-N(5)	86.58(18)
N(2)-Ni(1)-N(8)	84.47(17)	N(11)-Ni(1)-N(8)	89.60(18)
N(2)-Ni(1)-S(2)	92.67(12)	N(11)-Ni(1)-S(2)	85.98(14)
N(5)-Ni(1)-N(8)	155.85(17)		

Table 9: Continuous Shape Mapping Results for complexes **3**.

Structure	(HP-6)	(PPY-6)	(OC-6)	(TPR-6)	(JPPY-6)
3	31.376	23.400	1.969	11.013	27.458

HP: Hexagon (D_{6h}), PPY: Pentagonal pyramid (C_{5v}), OC: Octahedron (O_h), TP: Trigonal Pyramidal (D_{3h}), JPPY: Johnson's pentagonal pyramid J2 (C_{5v}).

[Zn^{II}L^1][ClO$_4$]$_2$·CH$_3$CN·CHCl$_3$ (5): The zinc compound crystallises in the orthorhombic space group Pccn and contains one complex within the asu (Fig. 7). The Zn^{II} cation lies at the centre of a slightly distorted trigonal bipyramid geometry (Table 10 and 11) and reveals a completely different co-ordination environment to the related Mn^{II} and Ni^{II} complexes. There are three equatorial nitrogen donors (N2, N5 and N8) which are located on the pyridyl groups with the bridge-head nitrogen (N1) and a sulfur donor occupying axial positions. The co-ordinative bond lengths vary from 2.106-2.165(6) Å for Zn-N bonds while the Zn-S bond is 2.3461(19) Å which, again, is almost identical to that observed in [Zn**L**^{2}][ClO$_{4]2.}$^{22} While some hydrogen bonding is observed in structure (Figure 8; Table 12), the perchlorate ion does not interact with all three thiourea groups of the ligand in the solid state.

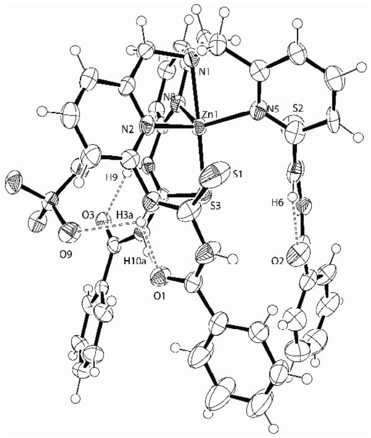

Figure 7: The asymmetric unit of **5.** Displacement ellipsoids are shown at 50% probability. H atoms are of arbitrary size.

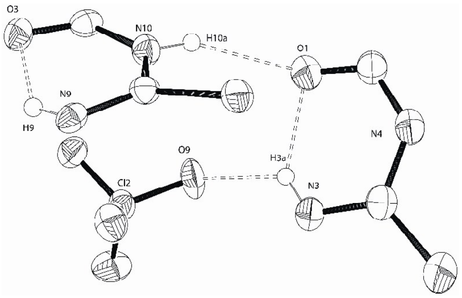

Figure 8: view of the hydrogen bonding interactions of **5**.

Table 10: Selected Bond lengths (A°) and Angles (°) for **5**

Zn(1)-N(1)	2.165(6)	Zn(1)-N(8)	2.150(6)
Zn(1)-N(2)	2.106(6)	Zn(1)-S(3)	2.3461(19)
Zn(1)-N(5)	2.111(6)		
N(1)-Zn(1)-S(3)	165.51(17)	N(5)-Zn(1)-N(1)	78.7(2)
N(2)-Zn(1)-N(1)	78.6(2)	N(5)-Zn(1)-N(8)	123.0(2)
N(2)-Zn(1)-N(5)	115.7(2)	N(5)-Zn(1)-S(3)	107.96(17)
N(2)-Zn(1)-N(8)	108.0(2)	N(8)-Zn(1)-N(1)	76.1(2)
N(2)-Zn(1)-S(3)	108.67(16)	N(8)-Zn(1)-S(3)	89.64(16)

Table 11: Continuous Shape Mapping Results for **5**.

Structure	(PP)	(VOC)	(TBPY)	(SPY)	(JSPY)	(JTBP)
Zn (**5**)	34.445	6.547	2.554	5.013	6.547	4.134

PP: Pentagon (D_{5h}), VOC: Vacant octahedron (C_{4v}), TBPY: Trigonal bipyramid (D_{3h}), SPY: Square pyramid (C_{4v}), JSPY: Johnson square pyramid (C_{4v}), JTBP: Johnson trigonal bipyramid (D_{3h}).

Table 12: H-bonding geometry (Å) for **5**

D-H…A	D-H	H…A	D…A	D-H…A
N3-H3A …O1	0.88	1.921	2.610	133.94
N6-H6...O2	0.88	1.930	2.608	132.59
N9-H9...O3	0.88	1.926	2.634	136.45
N3-H3A…O9	0.88	2.393	3.044	131.04
N10-H10A…O1	0.88	2.236	3.058	155.37

[Cd^{II}L^1][ClO$_4$]$_2$.0.5H$_2$O (6): The cadmium compound crystallises in the trigonal space group R-3 and contains 1/3 complex within the asu (Fig.9). The cadmium ion is surrounded by seven donor atoms (four N atoms and three S atom) and lies at the centre of a slightly distorted capped octahedron co-ordination geometry (Table 5). The nitrogen donor atoms are from the three pyridyl groups (N2, N2^i and N2^{ii}) and the bridging N1, while the other three co-ordinating atoms are sulfurs. This is the first example of crystallographically characterised co-ordination sphere involving N4S3 around a cadmium centre. The bond lengths between the pyridyl N-donors and the central Cd^{II} cation are listed in Table 13 and are slightly longer than those in the bisthiourea complex^{22} (2.497(4) compared to an average of 2.384(4) Å). In addition, while the average Cd-S distances are very similar in the two complexes, the bisthiourea complex has an asymmetric arrangement with one long and one short Cd-S bond. The complex has a very similar ligand arrangement as that observed with Mn(II). Similar to the Mn complex, one ClO$_4^-$ is observed in the central ligand cavity hydrogen bonding to three NH groups of the three thioureas. (Figure 10, Table 14)

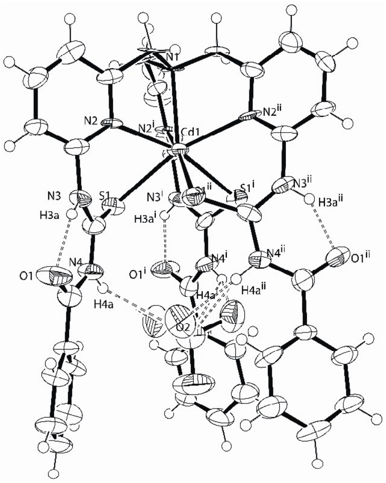

Figure 9 The asymmetric unit of **6**. Displacement ellipsoids are shown at 50% probability. H atoms are of arbitrary size.

Initial Qualitative Anion Binding Investigation

Attempts to obtain crystals of these complexes with different anions did not yield crystalline products. However, ^{31}P-NMR in CD_3CN was used to investigate whether the phosphate is interacting with the complex in solution. Fig. 11 shows that a small shift of 3.5 ppm is observed when a phosphate ion is added to **6** (compared to free phosphate)**,** while no notable shift was observed when phosphate was added to $[Cd^{II}(TPPA)]^{2+}$. Also, the addition of phosphate to the Zn comlex, **5**, did not result in a shift in the PO_4^{3-} peak in the ^{31}P NMR. For all ^{31}P NMR experiments, an insert of tetrabutyl ammonium phosphate was used to ensure consistent referencing of the spectra. This initial experiment confirms that the phosphate ions interacts with the cadmium complex. Future work will differentiate the ability of the different metal ions to bind the phospahte anion and quantify the strength of these interactions.

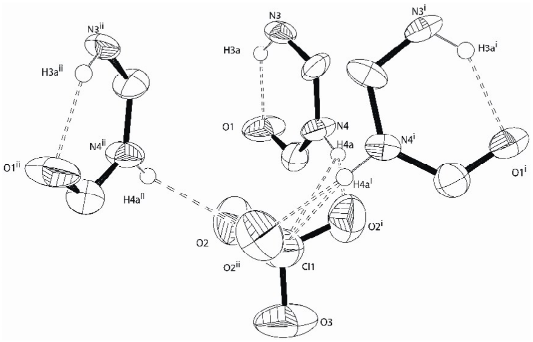

Figure 10: View of the hydrogen bonding interactions of **6**.

Table 13: Selected Bond lengths (A°) and Angles (°) for **6**

Cd(1)-N(1)	2.401(7)	Cd(1)-S(1)	2.6621(14)
Cd(1)-N(2)	2.497(4)		
N(1)-Cd(1)-N(2)	71.29(12)	N(2)-Cd(1)-S(1)^{i}	79.07(10)
N(1)-Cd(1)-S(1)	124.13(4)	N(2)-Cd(1)-S(1)^{ii}	164.49(13)
N(2)-Cd(1)-N(2)^{i}	110.22(11)	S(1)-Cd(1)-S(1)^{i}	91.60(5)
N(2)-Cd(1)-S(1)	76.46(10)		

Table 14: H-bonding geometry (Å) for **6**

D-H…A	D-H	H…A	D…A	D-H…A
N3-H3A …O1	0.88	1.848	2.575	138.61
N4-H4A …O5	0.88	2.135	2.953	154.26

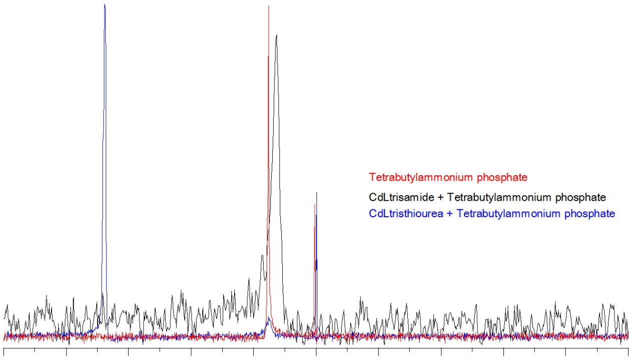

Figure 11: Superimposed ^{31}P NMR spectra of $(Bu_4N)_3PO_4$ (TBAP) (red), $[Cd(TPPA)]^{2+}$ [23] + TBAP (black) and **6** + TBAP (blue) complexes in CD_3CN. An insert of tetrabutylammonium phosphate in H_2O was used in all measurements as a reference.

Conclusions

The co-ordination chemistry of L^1 shows significant variations as the metal centre is changed. Several observations are worth noting:

The geometry of the complexes of L^1 and L^2 for a given metal ion is similar, with identical co-ordination numbers being observed. Mn(II) and Cd(II) yields 7 co-ordinate complexes, Ni(II) yields octahedral complexes and Zn(II) yields five co-ordinate complexes.

When five co-ordinate zinc species are obtained, both L^1 and L^2 co-ordinate by five of the seven or six available donors, with only one of the sulfur atoms co-ordinating to the metal centre.

The Ni(II) ion has a strong octahedral preference, forming octahedral complexes in both cases. Both ligands, again, only co-ordinate through five donor atoms. With L^1, only one of the sulphur donors coordinate to the metal centre, resulting in an unsymmetrical arrangement of the thiourea hydrogen bond donors and the C_3 symmetric hydrogen-bond donor cavity is *not* formed. The resulting complex is not predisposed to interacting with tetrahedral anions, unlike the Mn(II) and Cd(II) complexes. Such behaviour may offer a mechanism by which anion binding of a tetrahedral anion may be modified as the cation is swapped between nickel and manganese, for example.

Both Mn(II) and Cd(II) complexes form seven coordinate, monocapped octahedral complexes, with little distortion towards other geometries (Table 5). Neither Mn(II) (HS) and Cd(II) metal ions exert a geometrical preference and their structures are largely dictated by the steric preference of the ligand. The symmetrical arrangement of the NH bonds of the thiourea are arranged in a manner which allows multiple hydrogen bonds to be formed with a tetrahedral oxyanion (for example). While Zn(II), also a d^{10} metal, has no geometrical preference, it has a much smaller ionic radii, unsuited to the ligand cavity formed when L^1 is acting a septadentate ligand.

In the case of Zn(II), it is clearly more favourable to form a five co-ordinate trigonal bipyramidal structure, with only one of the three sulfur donors co-ordinated.

Future work will focus on the quantification of the hydrogen bonding interactions within these complexes and an investigation of how these interactions may be modified by the addition of a second metal or by a change in the metals oxidation state.

Acknowledgements

The authors would like to thank Institute of Scientific Research and Revival of Islamic Heritage at Umm Al-Qura University (Project ID 43305004) for financial support.

References:

1. T. Gunnlaugsson, M. Glynn, G. M. Tocci, P. E. Kruger and F. M. Pfeffer, *Coord. Chem. Rev.*, 2006, **250**, 3094-3117.
2. M. H. Filby and J. W. Steed, *Coord. Chem. Rev.*, 2006, **250**, 3200-3218.
3. C. R. Bondy and S. J. Loeb, *Coord. Chem. Rev.*, 2003, **240**, 77-99.
4. E. J. O'Neil and B. D. Smith, *Coord. Chem. Rev.*, 2006, **250**, 3068-3080.
5. A. N. Khlobystov, A. J. Blake, N. R. Champness, D. A. Lemenovskii, A. G. Majouga, N. V. Zyk and M. Schröder, *Coord. Chem. Rev.*, 2001, **222**, 155-192.
6. H. M. Chawla and S. P. Singh, *Tetrahedron*, 2008, **64**, 741-748.
7. 21. C.R. Rice, *Coord. Chem. Rev.* 2006, **250**, 3190.
8. P.D. Beer, P.A. Gale, *Angew. Chem. Int. Ed.*, 2001, **40**, 486.
9. L.C. Gilday, S.W. Robinson, T.A. Barendt, M.J. Langton, B.R. Mullaney, P.D. Beer, *Chem. Rev.*, 2015, **115**, 7118.
10. G.T. Spence, P.D. Beer, *Acc. Chem. Res.*, 2013, **46**, 571.
11. A. Caballero, F. Zapata, P.D. Beer, *Coord. Chem. Rev.*, 2013, **257**, 2434.
12. J.-F. Ayme, J.E. Beves, C.J. Campbell, G. Gil-Ramirez, D.A. Leight, A.J. Stephens, *J. Am. Chem. Soc.*, 2015, **137**, 9812.
13. A. Barnard, S.J. Dickson, M.J. Paterson, A.M. Todd, J.W. Steed, *Org. Biomol. Chem.*, 2009, **7**, 1554.
14. E. J. Cho, B. J. Ryu, Y. J. Lee and K. C. Nam, *Org. Lett.*, 2005, **7**, 2607-2609.
15. S. Camiolo, P. A. Gale, M. B. Hursthouse, M. E. Light and C. N. Warriner, *Tetrahedron Lett.*, 2003, **44**, 1367-1369.
16. E. Quinlan, S. E. Matthews and T. Gunnlaugsson, *J. Org. Chem.*, 2007, **72**, 7497-7503.
17. D. H. Lee, J. H. Im, J.-H. Lee and J.-I. Hong, *Tetrahedron Lett.*, 2002, **43**, 9637-9640.
18. D. A. Jose, D. K. Kumar, B. Ganguly and A. Das, *Tetrahedron Lett.*, 2005, **46**, 5343-5346.
19. (a) S. Moerkerke, S. Le Gac, F. Topic, K. Rissanen, I. Jabin, *Er. J. Org. Chem.*, 2013, 5315; (b) E. Brunetti, J.-F. Picron, K. Flidrova, G. Bruylants, K. Bartik, I. Jabin, *J. Org. Chem.*, 2014, **79**, 617, and references there in.
20. S. Moerkerke, J. Wouters, I. Jabin, *J. Org. Chem.*, 2015, **80**, 8720.
21. T.N. Lambert, B.D. Smith, *Coord. Chem. Rev.* 2003, **240**, 129.
22. F. A. Saad, N. J. Buurma, A. J. Amoroso, J. C. Knight and B. M. Kariuki, *Dalton Trans.* 2012, **41**, 4608.
23. F.A. Saad, J.C. Knight, B.M. Kariuki, A.J. Amoroso; *Dalton Trans.*, 2013, **42**, 14826.
24. M. Harata, K. Jitsukawa, H. Masuda and H. Einaga, *Chem. Lett.*, 1995, 61-62.
25. K. Jitsukawa, M. Harata, H. Arii, H. Sakurai and H. Masuda, *Inorg. Chim. Acta*, 2001, **324**, 108-116.
26. M. Sukeri, M. Yusof, S. Kamilah, C. Soh, N. Ngah and B. M. Yamin, *Acta Cryst. Section E*, 2006, **62**, 1446-1448.
27. M. G. B. Drew, J. Nelson, F. Esho, V. McKee and S. M. Nelson, *J. Chem. Soc., Dalton Trans.*, 1982, 1837 - 1843.
28. P. Dapporto, G. De Munno, A. Sega and C. Mealli, *Inorg. Chim. Acta*, 1984, **83**, 171-176.
29. A. Deroche, I. Morgenstern-Badarau, M. Cesario, J. Guilhem, B. Keita, L. Nadjo and C. Houee-Levin, *J. Am. Chem. Soc.*, 1996, **118**, 4567-4573.
30. C.-L. Chuang, K. Lim, Q. Chen, J. Zubieta, J.W. Canary, *Inorg. Chem.*, 1995, **34**, 2562; C.-L. Chuang, O. dos Santos, X. Xu, J.W. Canary, *Inorg. Chem.*, 1997, **36**, 1967.
31. R. Blessing, *Acta Cryst. Section A*, 1995, **51**, 33-38.
32. A. Altomare, G. Cascarano, C. Giacovazzo and A. Guagliardi, *J. App. Cryst.*, 1993, **26**, 343-350.
33. G. M. Sheldrick, *SHELXL-97, University of Göttingen, Germany*, 1997.
34. L. Farrugia, *J. App. Cryst.*, 1997, **30**, 565.
35. S. L. Tobey and E. V. Anslyn, *Org. Lett.*, 2003, **5**, 2029-2031.

Table 4: Crystal Structure Data for 1, 3, 5 and 6

Compound	Chemical formula	Colour/shape	Coordination number	Geometry	*Mw, g/mol*	Crystal system	Space group	T(K)	a, Å	b, Å	c, Å	α, deg	*β, deg*	γ, deg	V, Å3	Z	Observed Reflections	Unique Reflections	R_{int}	R_1 [I>2σ(I)]	wR_2 (all data)
1	$MnC_{44}H_{39}N_{11}O_{11}S_3Cl_2$	Colourless/ plate	7	Capped octahedron	1119.88	Trigonal	R-3:h	293(2)	13.7370(4)	13.7370(13)	44.1110(15)	90	90	120	7208.8(5)	6	1324	2831	0.1933	0.0739	0.1636
3	$NiC_{51.2}H_{50.6}N_{14.6}O_{11.4}Cl_2S_3$	Green/ needle	6	Octahedron	1278.65	Triclinic	P-1	293(2)	13.8450(5)	14.6430(5)	15.8030(6)	107.831(2)	97.828(2)	94.342(2)	2997.95(19)	2	6566	13501	0.1043	0.0931	0.2617
5	$ZnC_{45}H_{40}N_{11}O_{11}Cl_5S_3$	Colourless/ needle	5	trigonal bipyramid	1249.68	Orthorhombic	Pccn	150(2)	30.5910(3)	19.7950(3)	17.5370(5)	90	90	90	10619.5(4)	8	5486	8397	0.0869	0.0853	0.2283
6	$CdC_{42}H_{36.5}N_{10}O_{11.25}Cl_2S_3$	Colourless/ plate	7	Capped octahedron	1140.79	Trigonal	R-3:h	150(2)	13.8780(17)	13.8780(17)	43.257(8)	90	90	120	7215(2)	6	1023	2976	0.1195	0.0765	0.1522

Graphical Abstract

Co-ordination Behaviour of a Novel Tristhiourea Tripodal Ligand; Structural Variations in a Series of Transition Metal Complexes

Fawaz A. Saad,[a,b] James C. Knight,[a] Benson M. Kariuki[a] and Angelo J. Amoroso.[a]*

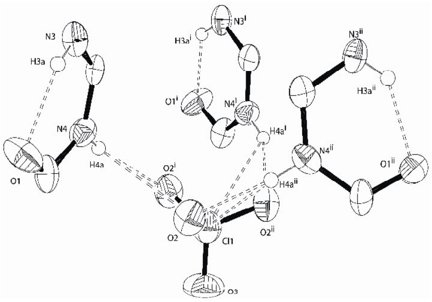

L^1 can potentially form a symmetrical array of hydrogen bond donors, suitable for the binding of tetrahedral anions. Data shows large metal ions, with no geometrical preferences, (Mn(II) and Cd(II)), form symmetrical seven co-ordinate monocapped octahedral complexes. Smaller metal ions (Zn(II)) favour asymmetric five co-ordinate trigonal bipyramidal structures while Ni(II) gives octahedral structures.